Journal of Alloys and Compounds 508 (2010) 528–531

Contents lists available at ScienceDirect

Journal of Alloys and Compounds

journal homepage: www.elsevier.com/locate/jallcom

Rotation-field annealing effect on magnetoimpedance of Co-based amorphous ribbons

S.U. Jen[a,b,*], H.P. Chiang[a,b], H.D. Liu[a,b], C.C. Chang[a]

[a] Institute of Physics, Academia Sinica, Taipei 11529, Taiwan, ROC
[b] Institute of Optoelectronic Sciences, National Taiwan Ocean University, Keelung 202, Taiwan, ROC

ARTICLE INFO

Article history:
Received 15 April 2010
Received in revised form 2 August 2010
Accepted 16 August 2010
Available online 22 September 2010

PACS:
75.60.Nt
72.15.Gd
75.50.Kj

Keywords:
Field-annealing
Magnetoimpedance
Co-based amorphous ribbon

ABSTRACT

A new annealing method, called the RFA method, is introduced to improve the magnetoimpedance (MI) effect in Co-based amorphous ribbons; e.g. VAC6025. This method includes applying a sufficiently large rotating field h_R, with a frequency F from 1 to 100 Hz, when the ribbon sample has been at the annealing temperature T_A (from 160 to 280 °C) for 1 h, and then is field-cooled to room temperature. The best achievements are that: [I] after the F = 1 or 50 Hz and T_A = 200 °C RFA treatment, the maximum MI ratio $(\Delta Z/Z)_m$ = 72% and the maximum operating frequency f_m = 0.6 MHz; [II] after the F = 50 Hz and T_A = 160 °C RFA treatment, the maximum field sensitivity S_m = 4.5%/Oe and the highest figure of merit FOM = 1.8% MHz/Oe; [III] since both of the optimal T_As above are much lower than the crystallization temperature (T_X = 500 °C), the samples remain ductile after RFA. In conclusion, we believe that the RFA treatment can greatly improve the MI performance of the VAC6025 ribbons, since h_R, operating at T_A and/or below, can effectively randomize the magnetic anisotropy, and thereby reduce the effective (or average) anisotropy energy $\langle K \rangle$. This is equivalent to stating that the RFA method is effective in enhancing the permeability or the $\Delta Z/Z$ ratio of any amorphous ribbon sample, including VAC6025.

1. Introduction

Zero-magnetostriction Co-based amorphous ribbon, which is known to exhibit giant magnetoimpedance (GMI) effect [1,2], can be used as a highly sensitive current or field sensor [3]. Usually, before putting the material to good use, a certain kind of field-annealing treatment is needed. For example, Refs. [3,4] suggested field-annealing Co-based amorphous ribbon at temperature T_A = 380 °C, near its crystallization temperature T_X, for 8 h in open air. The objective is that after their field-annealing treatments a surface crystallization and/or oxidation layer could be formed on the ribbon. As a result, a large asymmetric GMI is caused by the magnetic coupling between surface crystalline and inner amorphous phases. The advantage of this method is that the biasing field H_b can be drastically shifted or reduced, which means that although the maximum GMI, $(\Delta Z/Z)_m$, is only 15%, the field sensitivity is very high, about 35%/Oe. However, the disadvantages are that [I] the ribbon is brittle, and [II] the electrical resistivity, ρ, becomes smaller due to surface crystallization, which means that $(\Delta Z/Z)_m$ will occur at a lower operating frequency, such as f = 100 kHz. In this paper, we introduce a different field-annealing method. That is while annealing the ribbon at T_A, instead of applying a static dc field, we apply a rotation field, h_R, with various rotating frequency F in the ribbon plane. The hope was that through rotation-field annealing (RFA), we might randomize the anisotropy, thereby reducing the effective (or average) anisotropy energy, $\langle K \rangle$, in the ribbon, so that $(\Delta Z/Z)_m$ could be enhanced and H_b reduced at the same time. In addition, as shown below, the RFA method does not require high T_A, and the sample is not crystallized, or even embrittled [5]. As a result, besides the advantage of achieving a reasonably high sensitivity, the Co-based ribbon is still ductile after RFA, and can be operated under a bent (or twisted) condition [4,5].

2. Experiments

Nearly zero magnetostrictive Co-based amorphous ribbon, i.e. VAC6025 ($Co_{66}Fe_4Mo_2B_{11.5}Si_{16.5}$), was purchased from Goodfellow Cambridge Ltd. Each rectangular sample, with dimensions of 21 mm (L: length) × 2.2 mm (w: width) × 0.0225 mm (t: thickness) was cut from the ribbon spool. The as-cast sample was a fresh sample without any annealing treatment. All the other samples were subjected to specific field-annealing treatments. The RFA method includes annealing each ribbon sample at T_A = 160, 200, 240, and 280 °C in a vacuum of 1×10^{-6} Torr. Note that T_X of VAC6025 is 500 °C [6], much higher than the T_As used here. As shown in Fig. 1(a), there were four kinds of field-annealing treatments after the $T = T_A$ condition was reached. First, we had h = 0 Oe for the 1 h annealing. Second, we applied a dc (or static) longitudinal field $h = h_{\parallel}$ along the length of the sample during annealing, followed by field-cooling. Third, a dc transverse field $h = h_{\perp}$ was applied along the width during annealing, followed by field-cooling. Fourth, a rotating field $h = h_R \times e^{-i\Omega t} = h_{\parallel}(t) + ih_{\perp}(t)$, where $\Omega = 2\pi F$ and F = 1, 5, 10, 50, and 100 Hz was applied parallel to the plane of the sample during annealing, followed by field-

* Corresponding author at: Institute of Physics, Academia Sinica, Taipei, Nankang 11529, Taiwan, ROC. Tel.: +886 2 2789 6707; fax: +886 2 2783 4187.
E-mail address: physjen@gate.sinica.edu.tw (S.U. Jen).

0925-8388/$ – see front matter © 2010 Elsevier B.V. All rights reserved.
doi:10.1016/j.jallcom.2010.08.110

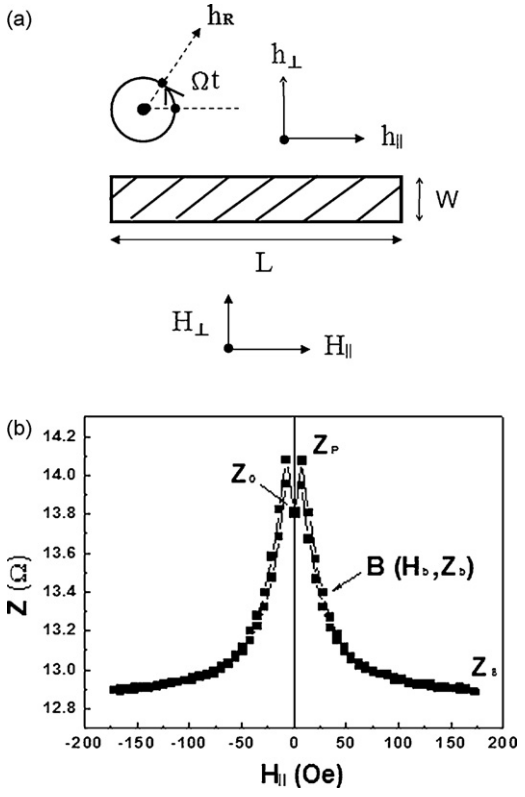

Fig. 1. (a) The rotation-field annealing and the magnetoimpedance (MI) test configurations. h_R, $h_\parallel$, or $h_\perp$ is the rotating, static longitudinal, static transverse field applied during anneal at T_A. $H_\parallel$ or $H_\perp$ is the external longitudinal or transverse field applied in the MI test. L is the length and w is the width of the ribbon sample. (b) A typical field ($H_\parallel$) dependence of MI in an annealed VAC6025 ribbon. Frequency f of the ac probe current was 1 MHz. $\Omega = 2\pi F$, where F is the rotating frequency of h_R.

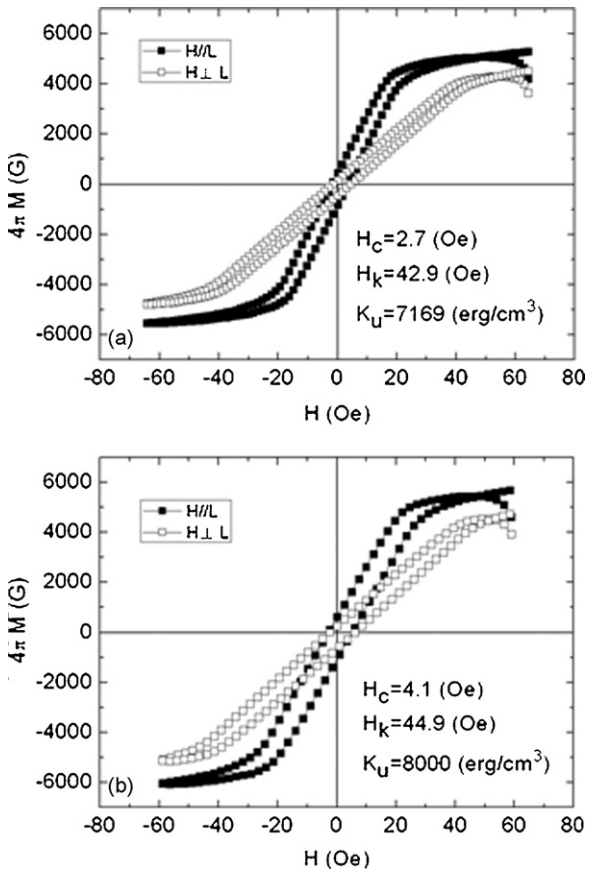

Fig. 2. Magnetic hysteresis loops of (a) the $T_S = 200\,^\circ$C and $h = h_R$ (RFA) ribbon sample and (b) the $T_S = 200\,^\circ$C and $h = h_\parallel$ (dc annealing field along the length L as shown in Fig. 1(a)) ribbon sample. H is the external field, H_C is the easy-axis coercivity, H_K is the hard-axis anisotropy field, and $K_u \equiv \langle K \rangle$ is the uniaxial anisotropy energy.

cooling. We roughly estimated the longitudinal and transverse demagnetizing fields, $H_D(L)$ and $H_D(W)$ at each T_A as shown in Table 1, to ensure that $h_\parallel$, $h_\perp$, and h_R (about 40 Oe) were sufficiently larger than those H_Ds.

The magnetoimpedance (MI) measurements were carried out using a HP4284A precision LCR Meter (in the f range 1 kHz–1 MHz) and an Agilent E4991A RF impedance/material analyzer (1 MHz–1 GHz), respectively at room temperature. The ac probe current sent through the sample was 4.8 mA. The impedance of the testing leads was nullified for each f. A pair of Helmholtz coils was used to apply an external longitudinal ($H_\parallel$) or transverse ($H_\perp$) field on the ribbon sample, as shown in Fig. 1(a). A typical Z versus $H_\parallel$ plot of the $h = 0$ sample at $f = 10$ MHz is shown in Fig. 1(b). $|H_\parallel|$ increases from Z_0 to Z_p, and then decreases to Z_S. This dip ($Z_p - Z_0$) phenomenon becomes more apparent when f is higher. The MI ratio is defined as $\Delta Z/Z \equiv (Z_p - Z_S)/Z_S$, and the sensitivity as $S \equiv (dZ/dH)_b(1/Z_b)$ at the inflection (or biasing) point B, as shown in Fig. 1(b). The dc electrical resistivity (ρ) was measured with the standard four-probe method. The magnetic easy- and hard-axis hysteresis loops of each ribbon sample were measured by a vibration sample magnetometer.

3. Results and discussion

As mentioned in Section 1, the idea of employing the RFA method is to reduce the effective $\langle K \rangle$ in the ribbon sample. Notice that due to the difference between $H_D(L)$ and $H_D(W)$, the easy-axis (EA) of the sample after the RFA treatment is along L, as in the case after the $h_\parallel$ treatment, but with $\langle K \rangle$ reduced in the former case. Fig. 2(a) and (b), where H_C is the easy-axis coercivity, H_K is the hard-axis anisotropy field, and $K_u \equiv \langle K \rangle$ is the uniaxial anisotropy energy, should confirm the arguments just made. Obviously, in the EA formation mechanism it is the internal annealing field, $h_i \equiv h - H_D$, that matters. Further, Refs. [7–10] show that the permeability μ_C at coercivity H_C (due to the domain wall motion) and the transverse permeability μ_T (due to magnetization M_S rotation) are related to $\langle K \rangle$ by the following relationships,

$$\mu_C \propto \frac{M_S^2}{\langle K \rangle}, \qquad \mu_T \propto \frac{M_S^2}{3\langle K \rangle} \tag{1}$$

In short, the permeability, μ_C or μ_T, is always inversely proportional to $\langle K \rangle$. From MI theory [11–13], when the eddy-current mechanism becomes effective, i.e. $Z_p \propto [\mu/\rho]^{1/2}$, where $\mu = \mu_C$

Table 1
T_A is the field-annealing temperature. $T_C = 250\,^\circ$C is the Curie temperature of VAC6025. RT = 23 °C stands for room temperature. M_S(RT) = 5.5 kG is the saturation magnetization at RT. $M_S(T_A)/M_S$(RT) is estimated according to the molecular field theory and Brillouin function $B_{1/2}(x)$. $N_d(L)$ and $N_d(w)$ are the demagnetizing factors along L and w. $H_d(L) = N_d(L) \times M_S(T_A)$ and $H_d(w) = N_d(w) \times M_S(T_A)$ are the longitudinal and transverse demagnetizing fields at each T_A.

T_A (°C)	T_A/T_C	$M_S(T_A)/M_S$(RT)	$M_S(T_A)$ (kG)	$N_d(L)\,10^{-4}$	$N_d(w)\,10^{-4}$	$H_d(L)$ (Oe)	$H_d(w)$ (Oe)
160	0.69	0.85	4.7	5.40	26.5	2.6	12.4
200	0.75	0.82	4.5	5.40	26.5	2.4	11.9
240	0.82	0.73	4.1	5.40	26.5	2.2	10.8
280	0.88	0.64	3.6	5.40	26.5	2.0	9.5
RT	0.48	1.00	5.5	5.40	26.5	3.0	14.5

Table 2
T_A is the field-annealing temperature. F is the frequency of the rotation field h_R during annealing. $h_\parallel$ and $h_\perp$ are the static longitudinal and transverse annealing fields. $(\Delta Z/Z)_m$ is the maximum MI ratio at frequency f_m. S_m is the maximum field sensitivity at f_S. FOM means figure of merit. ρ is the electrical resistivity.

T_A (°C)	Field	$(\Delta Z/Z)_m$ (%)	f_m (MHz)	S_m (%/Oe)	f_S (MHz)	FOM (% MHz/Oe)	ρ (μΩ cm)
200	$h = h_R$						
	$F = 1$ Hz	72	0.6	3.3	0.4	1.33	142
200	$F = 5$ Hz	69	0.6	2.7	0.4	1.10	129
200	$F = 10$ Hz	58	0.6	3.0	0.4	1.20	130
200	$F = 50$ Hz	72	0.6	3.5	0.4	1.40	135
200	$F = 100$ Hz	64	0.6	2.3	0.2	0.46	131
200	$h = h_\parallel$	52	0.6	1.5	0.8	1.20	117
200	$h = h_\perp$	48	0.6	1.4	0.4	0.56	117
200	$h = 0$	58	0.6	1.8	0.2	0.36	129
–	as-cast	34	0.6	1.8	0.4	0.72	119
	$h = h_R$						
160	$F = 50$ Hz	66	0.6	4.5	0.4	1.80	139
240	$F = 50$ Hz	68	0.6	2.0	0.6	1.20	115
280	$F = 50$ Hz	57	0.6	2.7	0.4	1.08	123

in the $H_\parallel$ and $h_\parallel$ case and $\mu = \mu_T$ in the $H_\parallel$ and $h_\perp$ case, and $Z_S \propto [\mu(H_S)/\rho]^{1/2}$, where H_S is the saturation field and $\mu(H_S) \ll \mu$, we find $\Delta Z/Z$ should be proportional to $\sqrt{\mu}$. Note that ρ does not play an important role here, since it does not change much after RFA (Table 2).

To summarize, three predictions can be made from Eq. (1). First, by reducing $\langle K \rangle$ with the RFA method as evidenced from Fig. 2, and thereby enhancing μ_C or μ_T, we can greatly improve the $\Delta Z/Z$ ratio. Second, $\mu_C > \mu_T$ from Eq. (1), $\Delta Z/Z$ in the case of $H = H_\parallel$ and $h = h_\parallel$ (the dc longitudinal anneal) is larger than that in the case of $H = H_\parallel$ and $h = h_\perp$ (the dc transverse anneal). Third, in the low f region, H_b is proportional to $H_C + H_D(L)$ in the $H = H_\parallel$ case and to $H_K + H_D(W)$, where $H_K = \langle K \rangle / [2\pi M_S]$ is the anisotropy field, in the $H = H_\perp$ case. In the high f region, the eddy-current effect enhances H_C or H_K so that H_b is an increasing function of f for both cases. Because we have $H_C < H_K$ and $H_D(L) < H_D(W)$ for all the samples, the biasing field H_b in the $H_\perp$ case is always larger than that in the $H_\parallel$ case for each sample. In addition, from a simple geometrical relationship in the $\Delta Z/Z$ versus $H_\parallel$ curve, it is easy to tell that $(dZ/dH)_b$ should be inversely proportional to H_b. As a result, S in the $H_\parallel$ case is also always larger than that in the $H_\perp$ case for each sample. Therefore, in Table 2 of this paper, we concentrate on the $H = H_\parallel$ results only.

Fig. 3 shows $\Delta Z/Z$ plotted as a function of f for the five kinds of samples: as-cast, $h = 0$, $h = h_\parallel$, $h = h_\perp$, and $h = h_R$ at $F = 50$ Hz. All the curves follow the same trend: $\Delta Z/Z$ first increases; then as f increases, $\Delta Z/Z$ reaches the maximum $(\Delta Z/Z)_m$ at $f = f_m = 0.6$ MHz (Table 2); thereafter $\Delta Z/Z$ decreases monotonically. This is in agreement with the GMI theory that f_m is roughly equal to the sample relaxation frequency $\omega_C/2\pi$, about 1 MHz [14]. From Fig. 1 and Table 2, we see that $(\Delta Z/Z)_m$ in the $F = 50$ Hz case is as high as 72%. This ratio is the highest, which is sufficient to fulfill our first prediction in the last paragraph. Next, $(\Delta Z/Z)_m = 52\%$ for the static $h = h_\parallel$ case is larger than $(\Delta Z/Z)_m = 48\%$ for the static $h = h_\perp$ case. This fact confirms our second prediction. $(\Delta Z/Z)_m = 58\%$ for the $h = 0$ case also shows that even with the zero-field annealing, the self-demagnetization field will automatically force the easy-axis parallel to L.

In Fig. 4, we show H_b plotted as a function of f for the (same) five kinds of samples (as in Fig. 1): the data in red are for the $H = H_\perp$ case, while those in black are for the $H = H_\parallel$ case. (For interpretation of the references to colour in this figure, the reader is referred to the web version of the article.) There are two features in Fig. 4. First, for all the samples, in the f range from 50 kHz to 0.1 GHz of Fig. 4, H_b in the $H_\parallel$ case is always smaller than the corresponding H_b in the $H_\perp$ case. Second, H_b increases monotonically, as f increases for both cases. These facts assert the third prediction.

Moreover, Fig. 5 shows the rotating frequency F effect on $(\Delta Z/Z)_m$. Once again, when $F = 0$, which corresponds to the static $h = h_\parallel$ case, $(\Delta Z/Z)_m$ is the lowest. Hence, Fig. 5 confirms that the RFA method with F in the range 1–100 Hz can improve $(\Delta Z/Z)_m$ with respect to the other static field-annealing methods. In addition, there are double peaks in the $(\Delta Z/Z)_m$ versus F plot: one occurs at $F = 1$ Hz, and the other at $F = 50$ Hz. The reason is unclear.

The S versus f plot is similar to the $(\Delta Z/Z)_m$ plot in Fig. 3; however, the position of the maximum sensitivity S_m occurs at $f = f_S$, different from f_m. This indicates that S_m is related not only to the f dependence of $(\Delta Z/Z)$, Fig. 3, but also to the f dependence of

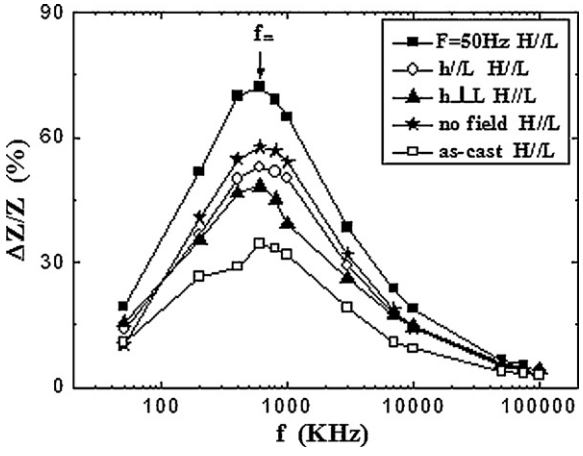

Fig. 3. The MI ratio $\Delta Z/Z$ of some VAC6025 ribbons plotted as a function of the ac probe current frequency f. At $f = f_m$, we have $(\Delta Z/Z)_m$ for each sample.

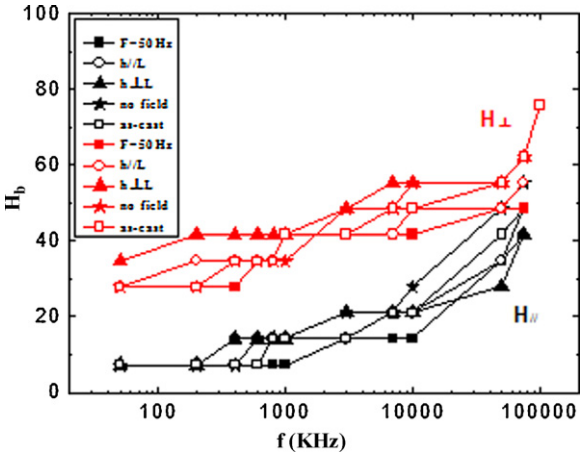

Fig. 4. The biasing field H_b, as defined in Fig. 1(b), is plotted as a function of f.

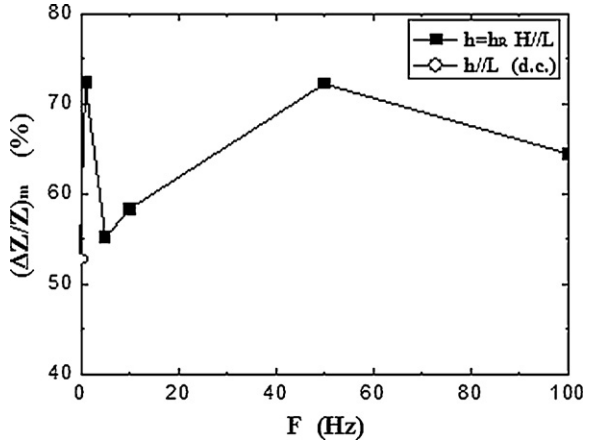

Fig. 5. The maximum MI ratio $(\Delta Z/Z)_m$, as defined in Fig. 3, is plotted as a function of the frequency F of the rotation field h_R during annealing at $T_A = 200\,^\circ C$.

H_b, Fig. 4. From Table 1, it is seen that when $T_A = 200\,^\circ C$ is fixed, $S_m = 3.5\%/Oe$ reaches the highest field sensitivity for the sample after the RFA treatment with $F = 50$ Hz. Further, we have tried various RFA (with different T_As but the same $F = 50$ Hz) treatments. From Table 2, we summarize the T_A results as follows: in the T_A range from 160 to 280 °C, we find $(\Delta Z/Z)_m$ reaches the maximum value, 72%, when $T_A = 200\,^\circ C$, and S_m reaches the maximum value, 4.5%/Oe, when $T_A = 160\,^\circ C$. These results indicate that [A] the low T_A RFA method is effective in improving the MI effect; and [B] when $T_A > 240\,^\circ C$, the effectiveness of the RFA method decreases. Result [B] is reasonable, since according to Ref. [6], the Curie temperature T_C of VAC6025 is 250 °C. Therefore, when $T_A = 280\,^\circ C > T_C$, VAC6025 becomes non-ferromagnetic, and the rotating field h_R is ineffective to the sample under this circumstance.

Finally, according to Ref. [15], the figure of merit (FOM) of the MI effect in amorphous ribbons is defined as $FOM \equiv S_m f_S$. From Table 2, the magnitude of FOM is the largest (1.80% MHz/Oe) for the VAC6025 ribbon sample after the RFA treatment with $T_A = 160\,^\circ C$ and $F = 50$ Hz. In contrast, if the ribbon sample has not been subjected to the RFA treatment, its FOM is only about 0.4–0.7% MHz/Oe.

4. Conclusion

We have introduced a new annealing method to improve the MI effect in the VAC6025 ribbons. This method includes applying a rotating field h_R with a frequency F when the ribbon sample has been heated at the annealing temperature T_A for 1 h and then field-cooled to room temperature. In terms of the $(\Delta Z/Z)_m$ improvement, when in the as-cast state, $(\Delta Z/Z)_m$ is only 34%, but after the rotation-field annealing (RFA) with $T_A = 200\,^\circ C$ and $F = 1$ or 50 Hz, $(\Delta Z/Z)_m$ reaches 72%. In terms of S_m and/or FOM improvements, for the as-cast sample, $S_m = 1.8\%/Oe$ and FOM = 0.7% MHz/Oe, while for the sample after RFA (with $T_A = 160\,^\circ C$ and $F = 50$ Hz), $S_m = 4.5\%/Oe$ and FOM = 1.8% MHz/Oe. Moreover, another important merit of using the RFA treatment is that it does not require high annealing T_A. Hence, the ribbon sample remains ductile (good mechanical property) after this annealing treatment.

Acknowledgement

We are thankful for the financial support from the National Science Council (Grant No. NSC97-2112-M-01-023-MY3).

References

[1] J.M. Barandiarán, A. Hernando, J. Magn. Magn. Mater. 268 (2004) 309.
[2] V.M. Prida, P. Gorria, G.K. Kurlyandskaya, M.L. Sanchez, B. Hernando, M. Tejedor, Nanotechnology 14 (2003) 231.
[3] P. Kollu, L. Jin, K.W. Kim, S.S. Yoon, C.G. Kim, Appl. Phys. A 90 (2008) 533.
[4] Y.W. Rheem, C.G. Kim, C.O. Kim, S.S. Yoon, Sens. Actuators A 106 (2003) 19.
[5] S.U. Jen, D.R. Huang, Chin. J. Phys. 24 (1986) 239.
[6] Data sheet issued by Vacuumschmelze GmbH.
[7] G. Buttino, A. Cecchetti, M. Poppi, J. Magn. Magn. Mater. 269 (2004) 70.
[8] G. Herzer, IEEE Trans. MAG-26 (1990) 1397.
[9] S.U. Jen, L. Berger, J. Appl. Phys. 53 (1982) 2298.
[10] S.U. Jen, T.L. Tsai, C.C. Lin, J. Appl. Phys. 106 (2009) 013901.
[11] L.V. Panina, K. Mohri, T. Uchiyama, M. Noda, IEEE Trans. MAG-31 (1995) 1249.
[12] S.U. Jen, Y.D. Chao, J. Appl. Phys. 79 (1996) 6552.
[13] T. Morikawa, Y. Nishibe, H. Yamadera, Y. Nonomura, M. Takeuchi, Y. Taga, IEEE Trans. MAG-33 (1997) 4367.
[14] L. Kraus, J. Magn. Magn. Mater. 196–197 (1999) 354.
[15] C.M. Cai, K. Mohri, Y. Honkura, M. Yamamoto, J. Magn. Soc. Jpn. 25 (2001) 967.